TECHNICAL UNIVERSITY OF CLUJ-NAPOCA

ACTA TECHNICA NAPOCENSIS

Series: Applied Mathematics, Mechanics, and Engineering
Vol. 58, Issue I, March, 2015

MECHANICAL MODEL OF THE CUTTING PROCESS IN STEEL FACING

Sorin ACHIMAŞ, Marian BORZAN, Florin MOCEAN,
Dorina (căs. BĂRĂIAN) PINTEA, Adrian TRIF

Abstract: In order to improve the metallic material cutting process, numerical modelling and simulation are applicable. One of the requirements is numerical modelling of the interaction at the tool-chip interface such as to predict the performance of cutting process. Cutting forces occur as a result of elastic and plastic deformation of the chip and processed surface, for breaking, detaching, additionally deforming (bending and curling) the chip, as well as to overcome the friction between the chip and the cutting face, and between the cutting face and processed surface.
Key words: facing, modelling, finite element, numerical simulation.

1. INTRODUCTION

Development of cutting tools and techniques of processing by cutting was mostly conditioned by the development of machine tools and various materials used for manufacturing such tools.

Figure 1 presents the evolution of cutting tools with the most significant steps. Quality of products made with cutting procedures, productivity as well as price of parts depend on the precision and quality of cutting tools.

Fig.1 Evolution of cutting tools [4]

Conception by Karl Schroter [5] of the tungsten carbide sintering in cobalt allowed for obtaining tool materials known as metal-ceramic materials or sinterized metallic carbides, with high performances.

Metal carbides currently used are obtained by sintering tungsten, titan and tantalum carbides using cobalt as a bonding agent. Mineral-ceramic materials have also been used, obtained by sintering Al2O3 aluminium oxide powder, either in pure state or mixed with metal carbides.

Recently, coated plates are being used, with a tungsten and cobalt carbide core, covered with a layer of titan carbide with a thickness of 2-4 µm, providing the hard alloy plate with high endurance to wear.

The latest achievements in the field of metal carbides are the double coated plates, obtained by coating the titan carbide layer with an aluminium oxide layer with a thickness around 1 µm. These plates can be used to process alloyed cast iron and steel (45 …70 HRC) both in finishing and thinning operations. Figure 2 presents the evolution of metal carbides plates with various types of coatings.

The fact that metal carbide plates presents high hardness and endurance to high temperatures, much higher than rapid steel, allowed for such knives to operate at substantially higher cutting speeds, which contributed to their development and diversification.

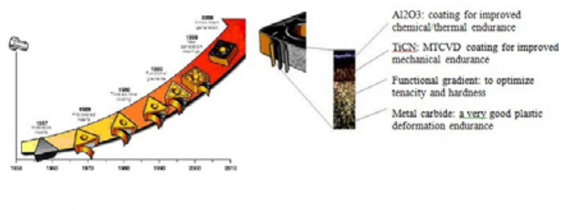

a) b)

Fig.2 Evolution of metal carbide coatings:(a) evolution of coatings; (b)types of structures[4]

2. ELEMENTS OF THE CUTTING PROCESS

When facing cylindrical parts, the part performs a rotational movement and the lathe knife travels parallel to the rotation axis of the processed part. Elements of the cutting process are:

- Main cutting velocity, determined with the equation:

$$v_p = \frac{\pi \times D \times n}{1000} \left[\frac{m}{min}\right] \quad (1)$$

where D is diameter of the part performing the main rotational movement, expressed in mm, and n is rotation speed in rev/min ;n – rotation frequency in rev/min.

- Advance movement, which removes successive layers of material in front of the tool's edge, determined with the equation:

$$v_s = \frac{s \times n}{1000} \left[\frac{m}{min}\right] \quad (2)$$

where s represents advance per revolution.

- Tool's constructive angles;
- Tool wear, which depends on several factors: parameters of cutting process, part material, tool material etc.

$$u_r = C_u \cdot v^m \cdot s^n \cdot t^p \cdot K_a \cdot K_g \cdot K_r \quad (3)$$

where : v [m/min] – cutting velocity; s [mm/rev] – working advance; t [mm] – cutting depth; C_u, m, n, p - constants depending on cutting parameters; K_a, K_g, K_r - coefficients describing the geometry of tool's cutting side (side relief angle α, rake angle γ and tip rounding radius r).

To be mentioned that tool wear calculated with equation (3) is just an approximation, in actual situations there are more factors affecting cutting velocity, calculated as per equation (1), and wear.

- Cutting force, total cutting force is calculated with equation [1] :

$$F = \sqrt{F_x^2 + F_y^2 + F_z^2} \quad (4)$$

- Cutting power is calculated with the equation:

$$P = \frac{F_z \cdot v_z}{6120} \text{ [kw]} \quad (5)$$

3. DEFINING THE RANGE OF ANALYSIS OF THE CUTTING PROCESS AND IDENTIFYING LIMITS

Analysis range will be selected as a small area of the part, located near the tool's cutting edge. For a two-dimensional analysis, the hypothesis to be adopted is that the chip width is large in comparison with the size of the previously selected area. From the mechanical point of view the problem will have characteristics which are specific to plane deformation. The analysis range with the adopted coordinates system is presented in figure 3. In fact, this area is a two-dimensional section which is oriented perpendicularly on the tool's cutting edge. Point E is the projection of the edge on the drawing plane. Z axis in the coordinates system corresponds to the view perpendicular on the drawing. Boundaries AB and EF are in fact circular. However, since the dimensions of analysed area are small compared to the part's diameter, they will be approximated as plane sides. Angle α is defined by tool geometry. Distance *h* represents length of contact between knife and chip [4]:

$$h = \frac{f \sin\theta}{\sin\phi \cos(\theta + \alpha - \phi)} \quad (6)$$

where ø is the shearing angle (namely the gradient of shearing plane from the cutting direction), θ is the angle between the shearing component of the cutting force and the cutting force itself, and *f* is the advancement. In the case of orthogonal cutting, the shearing angle may be evaluated using ratio *r* defined below:

$$r = \frac{\sin\phi}{\cos(\phi-\alpha)} \qquad (7)$$

Furthermore, angle θ results from the equation:

$$\cos\theta = \frac{F_c\cos\phi - F_t\sin\phi}{\sqrt{F_c^2+F_t^2}} \qquad (8)$$

where F_c is cutting force, and F_t is the axial pushing force.

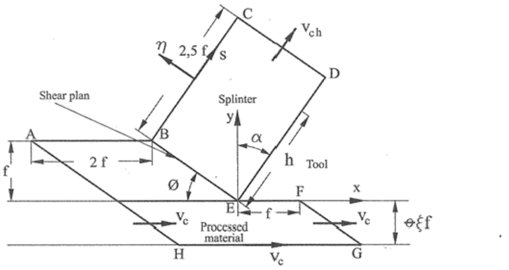

Fig.3. Range of analysis in numerical simulation of an orthogonal cutting process [6] , [4]

Boundaries AH, HG, FG and CD are located at sufficient distance from the projection of cutting edge E, thus a uniform distribution of velocities may be considered at their level. Also, as presented in figure 3, boundaries AH, FG and CD are parallel with the shearing plane. With this particular placement, generation of finite elements mesh is much simplified.

4. EQUATIONS OF THE CUTTING PROCESS MECHANICAL MODEL

Condition parameters of the material subject to cutting are velocities field **v**, deformation rates field $\acute{\varepsilon}$, pressure field *p* and deviatory tensions field σ'. These parameters are connected by the following relations:

- equations defining deformation rates field as depending on velocities field;
- constitutive equations defining pressure and deviatory tensions associated to a certain distribution of deformation rates;
- mechanical balance equations (Cauchy's equations);
- material volume conservation condition.

For the purposes of analysing a cutting process, the equations listed above have to be broken down on components. As the problem presents a two-dimensional character, velocities field **v** has only two components which are not null. As regards the $\acute{\varepsilon}$ and σ' fields they each have three not null components. Considering these aspects, the relations defining the mechanical model of the cutting process presented in figure 3 are as follows:

- equations defining the deformation rates field [$\acute{\varepsilon}_{xx}$, $\acute{\varepsilon}_{yy}$, $\acute{\varepsilon}_{xy}$] as a dependency to velocities field [v_x ,v_y] :

$$\dot{\varepsilon}_{yy} = \frac{\partial v_y}{\partial y},\ \dot{\varepsilon}_{xy} = \frac{1}{2}\left(\frac{\partial v_x}{\partial y} + \frac{\partial v_y}{\partial x}\right) \qquad (9)$$

- viscoplastic constitutive equations describing deviatory tensions [σ'_{xx} , σ'_{yy} , σ'_{xy}] associated to a certain distribution of deformation rates [$\acute{\varepsilon}_{xx}$, $\acute{\varepsilon}_{yy}$, $\acute{\varepsilon}_{xy}$]:

$$\sigma'_{xx} = 2\eta_2\, \acute{\varepsilon}_{xx},\ \sigma'_{yy}=2\eta_2\, \acute{\varepsilon}_{yy},\ \sigma'_{xy}=2\eta_2\, \acute{\varepsilon}_{xy}\,. \qquad (10)$$

In equations (5), parameter η_2 represents the viscoplastic non-linear behaviour of the processed part and is expressed as

$$\eta_2 = a\left(\dot{\varepsilon}_{eq}\right)^m + \frac{\sigma_y}{3\dot{\varepsilon}_{eq}} \qquad (11)$$

where σ_y is the material's yield point,

$$\dot{\varepsilon}_{eq} = \sqrt{\frac{2}{3}\left(\dot{\varepsilon}_{xx}^2 + \dot{\varepsilon}_{yy}^2 + 2\dot{\varepsilon}_{xy}^2\right)} \qquad (12)$$

is the equivalent deformation rate, and *a* and *m* are material specific constants.

To take into account the thermal effects of the cutting process, σ_y, *a* and *m* are evaluated for the average temperature of the cutting area.

- mechanical balance equations: as mentioned above, the analysis will ignore the inertial forces, considering that the cutting process runs in stationary regime. In such circumstances, the equations are expressed as:

$$\rho\left(v_x\frac{\partial v_x}{\partial x} + v_y\frac{\partial v_x}{\partial y}\right) = -\frac{\partial p}{\partial x} + \left(\frac{\partial \sigma'_{xx}}{\partial x} + \frac{\partial \sigma'_{xy}}{\partial y}\right),$$

$$\rho\left(v_x\frac{\partial v_y}{\partial x} + v_y\frac{\partial v_y}{\partial y}\right) = -\frac{\partial p}{\partial y} + \left(\frac{\partial \sigma'_{xy}}{\partial x} + \frac{\partial \sigma'_{yy}}{\partial y}\right) \qquad (13)$$

where ρ is the mass density of processed material (constant due to material volume conservation) .

- material's volume conservation condition is expressed as:

$$\dot{\varepsilon}_{xx} + \dot{\varepsilon}_{yy} = 0 \quad (14)$$

The system of equations with partial derivatives (9) + (14) will be accompanied by the following limit conditions:

- on boundaries AH, HG and FG (figure 3).

As mentioned above, boundaries AH, HG and FG are far enough from the cutting area such as to consider the distribution of velocities at their level as being uniform and characterised by a single not null component (ν_x). If ν_c is known cutting velocity, this allows for specifying the limit condition associated to boundaries AH, HG and FG as follows:

$$\nu_x = \nu_c , \nu_y = 0 \quad (15)$$

- on boundary CD (figure 3).

Boundary CD is also located far enough from the cutting area. Consequently, velocities at its level may be considered with a uniform distribution. Be:

$$\nu_{ch} = \nu_c r \quad (16)$$

Chip translation velocity (calculated with ratio *r* defined in equation (7)). Since ν_{ch} forms angle α with axis *y* – see figure 3, the limit condition associated to boundary CD will be expressed as follows:

$$\nu_x = \nu_{ch}\sin\alpha , \nu_y = \nu_{ch}\cos\alpha \quad (17)$$

- on boundaries AB, BC and EF (figure 3).

Boundaries AB, BC and EF correspond to areas free of loads. Consequently, at their level the limit condition requires null values:

$$t_x = 0 , t_y = 0 . \quad (18)$$

In certain cases, on boundaries AB, BC and EF may be applied other constraints. As the direction of velocity vector is always parallel to axis *x* at the level of boundaries AB and EF, this area allows for imposing mixed conditions:

$$t_x = 0 , \nu_y = 0 . \quad (19)$$

BC makes an angle with axis *x* – figure 3. Consequently, in this area the annulment of normal component of velocity (ν_n), and of tangent component of traction (t_s) may be imposed:

$$\nu_n = -\nu_x\cos\alpha + \nu_y\sin\alpha = 0 , t_s = t_x\sin\alpha + t_y\cos\alpha = 0 \quad (20)$$

In general, mixed conditions like (19) - (20) provide more accurate solutions than the homogenous alternative (18).

- on boundary ED (tool-chip interface) – figure 3.

Along boundary ED, distribution of velocity may be approximated with the equation

$$v_\xi = \begin{cases} \frac{v_{ch}}{3}\sqrt{1+8\frac{\xi}{h}}, \text{ pentru } \xi \le h \\ v_\xi = v_{ch}, \text{ pentru } \xi > h \end{cases} \quad (21)$$

where ξ is distance measured from current point to projection E of the cutting edge. As the segment ED makes angle α with axis *y* – figure 3, the limit condition associated to this boundary will be expressed as:

$$\nu_x = \nu_\xi\sin\alpha , \nu_y = \nu_\xi\cos\alpha . \quad (22)$$

components ν_x and ν_y of traction vector.

5. CASE STUDY

5.1 Removable inserts

SECO removable inserts are metric series and standardised as per ISO 1832-2004. Inserts coding is presented in figure 4 [13].

Fig. 5 Inserts coding:
1. shape of removable insert; 2. rake angle; 3. tolerance; 4. type; 5. length of cutting edge; 6. thickness; 7. tip radius; 8. edge direction; 9. version; 10. description (for rough cutting R, for medium M and for finishing F).

SECO range provides inserts covered with protective layers (C.V.D and P.V.D), with high contents of TiC – cermet as well as not covered.

Stainless steel is high alloy steel with Cr or Cr-Ni, the materials considered for study were mark x40Ci13 (martensitic steel with carbon contents of 0.4% and Cr contents of 13%) and mark x12CrNi 18.9 (austenitic steel with carbon contents of 0.12%, Cr contents of 18% and Ni contents of 9%).

Taking into consideration the cutting laws and the effect of parameters on tool wear, the sequence for determining the cutting regime is the following: cutting depth “t” in [mm]; advance “s” in [mm/rot]; main cutting speed, “v_p” in [m/min].

The elements of cutting regime have been selected according to the tools manufacturer, based on recommendations from specialised literature.

5.2 Interpreting the results

5.2.1 Comparison of results between rough cutting of x40Cr13 and x12CrNi 18.9 materials

From the menu “Simulate” select option “Run simulation” to start shaping process.

5.2.1.1 Determine part structure

Deterioration of part structure is presented in colour codes (Fig. 6), so for material x40Cr13 it reaches 0.154 units, while for material x12CrNi 18.9 is around 0.1 units.

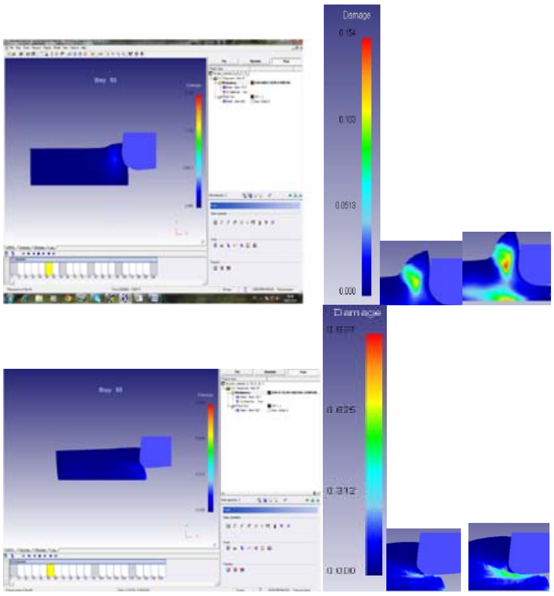

Fig.6 Determine part structure
a) for x40Cr13
b) for x12CrNi 18.9

5.2.1.2 Actual deformation

Deformability of metals and alloys represents their capacity to be permanently deformed without breaking internal links.

The amount of deformation applicable to a given material, without cracking or breaking it during deformation, at given temperature and deformation rate, is generally considered the material’s deformability.

Deformation for rough cutting material x40Cr13 was of 4.57 mm/mm, and for material x12CrNi 18.9 was of 3.84mm/mm.

5.2.1.3 Deformation rate

Deformation rate during cutting reaches a magnitude of tends and hundreds of meters per minute, the temperature in the cutting area is very high and variable, and the deformation level is high. In figure 7 the deformation rates for the two materials are presented.

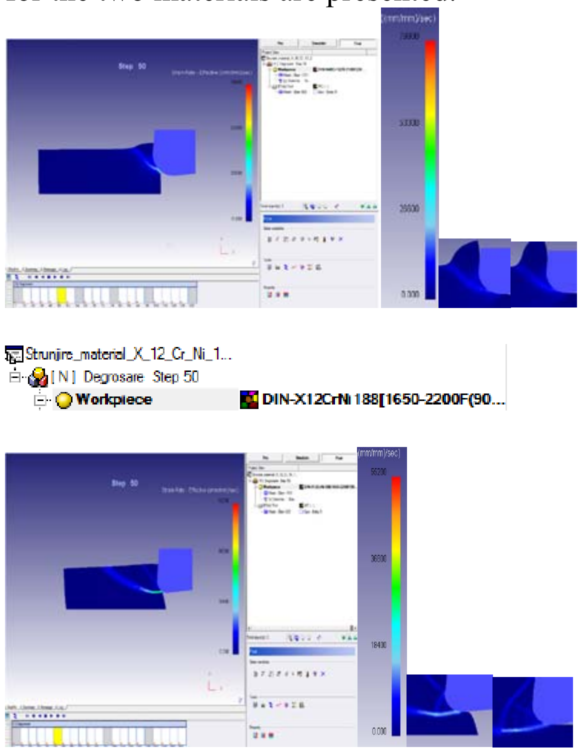

Fig. 7 Variation of deformation rate for cutting, expressed in mm/mm/sec:
a) material x40Cr13, rate of about 20,000;
b) x12 CrNi 18.9, about 18,400.

5.2.1.4 Tensions during processing

During the cutting process, the part is subject to mechanical tension.

The magnitude varies during different stages of processing. For material x40Cr13, tension reaches 800 Mpa, and for material x12CrNi 18.9 it reaches 781 Mpa.

5.2.1.5 Cutting speed

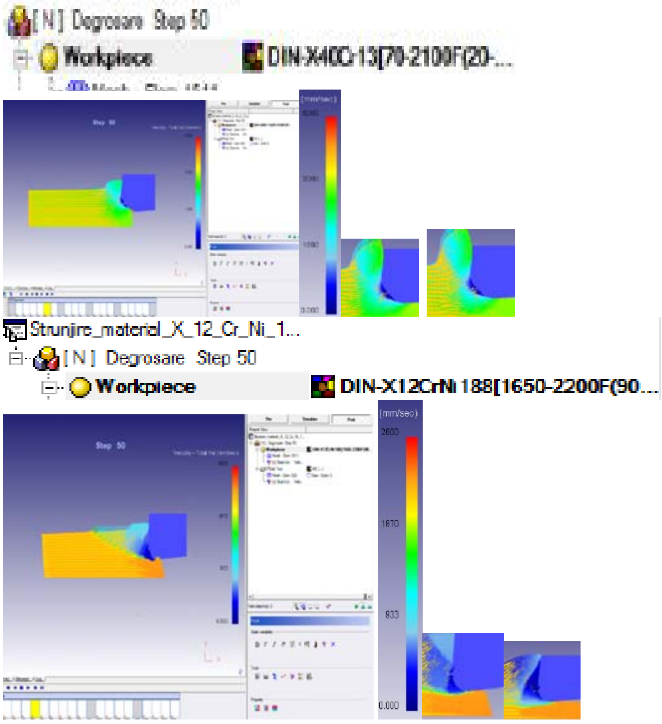

Fig.8 Cutting speed;
a) material x40Cr13
b) material x12CrNi 18.9

Cutting speed values were selected as recommended by the tool manufacturer, according to material's cutting class. For material x40Cr13 selected speed was of 195 mm/sec, and for x12CrNi 18.9 the speed was of 145 mm/sec. To be mentioned that the cutting speed is maintained constant during every cutting stage (Fig.8).

5.2.1.6 Normal pressure

Pressure represents the transmission of force or momentum from a part to the conjugated press through the surface of contact. Area of contact surface is constant, cutting force is approximately constant, and therefore the pressure value is constant during every stage of processing.

5.2.1.7 Temperature

Total mechanical work consumed during the cutting process is almost completely transformed into heat (only a small amount of work is stored as potential energy, namely internal tension, in the processed material).

Regarding the tool temperature, it will affect most parameters of cutting process, namely the part material, edge material, edge geometry, parameters of cutting regime, cooling-lubrication conditions (cutting media) etc. In figure 9 the temperature resulting during the cutting process is presented for the materials under study.

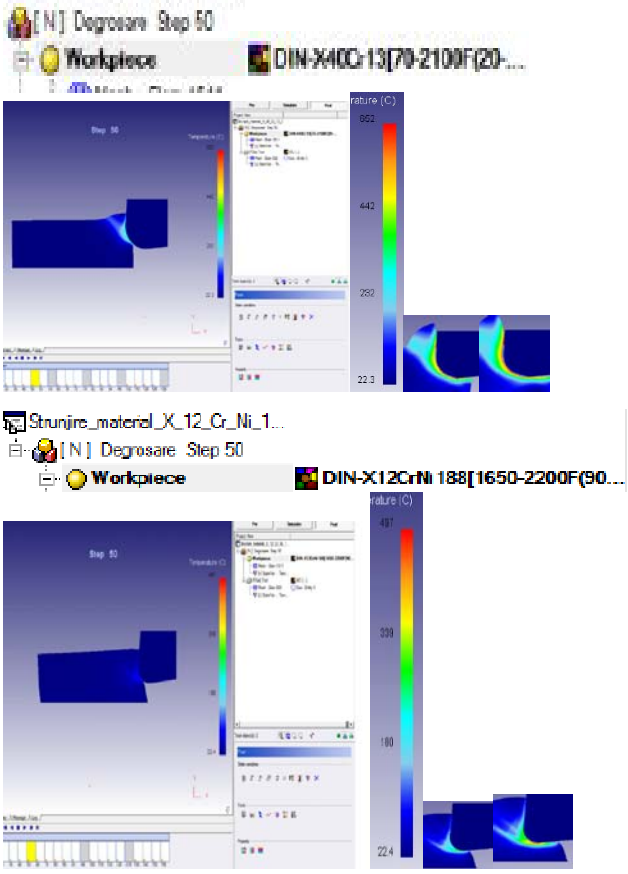

Fig. 9 Temperature achieved during cutting process: a) for material x40Cr13, temperature reaches 850^{0}C; b) for material x12CrNi 18.9, temperature reaches 487^{0}C.

5.2.2 Comparison of finish cutting for material x40Cr13 and material x12CrNi 18.9

5.2.2.1 Deterioration of material structure

Deterioration of material structure for x40Cr13 was of 0.242 units, and for material x12CrNi 18.9 was of 0.636.

5.2.2.2 Actual deformation

Deformation when finishing material x40Cr13 was of 3.18 mm/mm, and for material x12CrNi 18.9 was of 4.64 mm/mm.

5.2.2.3 Deformation rate

Deformation rate in mm/mm/sec for material x40Cr13 was approximately 100,000 mm/mm/sec, and for material x12CrNi 18.9 was approximately 80,000 mm/mm/sec.

5.2.2.4 Tension during processing

Figure 10 presents the variation of tension when finishing the metals under study.

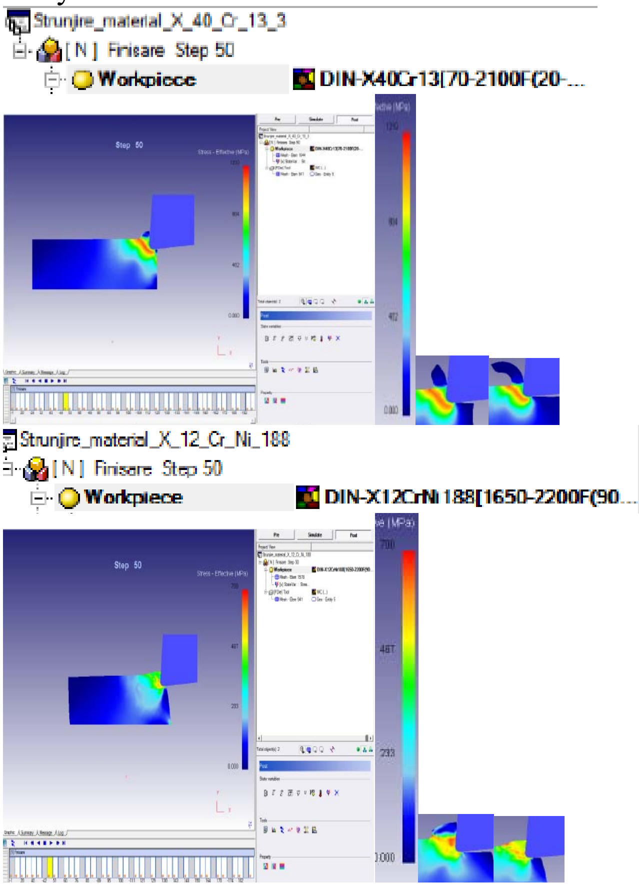

Fig. 10 Tension during finishing;
a) for material x40Cr13, tension value reaches 1000 MPa; b) for material x12CrNi 18.9, tension value reaches 700 MPa

5.2.2.5 Temperature

Generation of heat is a phenomenon inevitably associated with the cutting process.

It is produced by the almost complete transformation of mechanical work used for cutting; its intensity and the distribution of thermal flow determine the process temperature. This temperature has a decisive influence on the nature and dynamics of phenomena specific to the cutting process, such as chip formation and tool wear.

Figure 11 presents the variation of temperature during the cutting process for finishing the materials under study

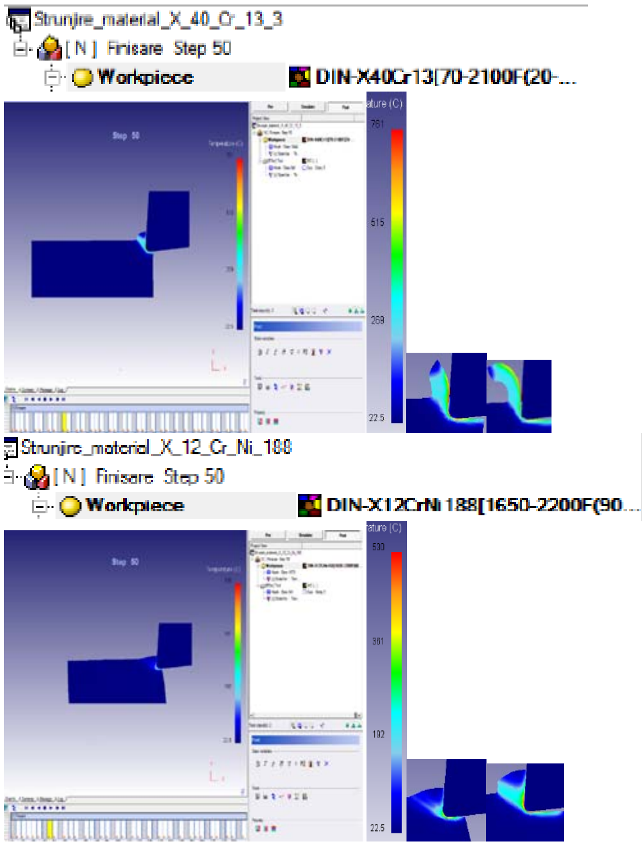

Fig. 11 Cutting temperature;
a) for material x40Cr13, reaches up to 761^{0}C;
b) for material x12CrNi 18.9, reaches up to 530^{0}C.

6. CONCLUSIONS

Results obtained by analysis with Finite Elements Method are determined both by performances of mechanical model and the mathematical principles and procedures in the finite elements method and software.

With the simulation software DEFORM 2D an orthogonal lathing process can be simulated. The cutting process simulation allows for monitoring temperature variation, normal pressure value, cutting velocity, chip deformation etc. Thus there is the possibility to optimise the parameters of cutting process which play a significant role in productivity and quality of processed surface.

Using the software application DEFORM 2DV 9.01, an orthogonal cutting process can be simulated and the process conditions can be defined for every stage of the process.

With this program, the temperature, normal pressure, cutting speed, tension, cutting forces occurring in the cutting area can be monitored.

ACKNOWLEDGEMENT: The present paper benefited from financial support under the project "1.5 Doctoral and post-doctoral programs supporting research", contract POSDRU/159 /1.5/5/134378, beneficiary "Transilvania" University in Braşov, project co-financed from the European Social Fund through the Sectorial Operational Program Development of Human Resources 2007-2013 and by the Government of Romania.

7.REFERENCES

[1] Borzan, M. Proiectarea sculelor profilate Editura Studium, Cluj-Napoca, 2001.
[2] Borzan, M. ş.a. Elemente de asigurarea si managementul calitatii. Editura Studium, Cluj-Napoca, 2001.
[3] Comşa, S. Metoda elementelor finite. Editura UT-PRES, Cluj-Napoca, 2007.
[4] Dixit, P.M.,Dixit. Modeling of Metal Forming and Machining Processes by Finite Element and Soft Computing Methods. Berlin: Springer, 2008.
[5] Julean, D. Aşchierea metalelor. Editura Dacia, Cluj-Napoca, 2000.
[6] Iwata, K.,Terasaka, Y. Process modelling of orthogonal cutting by rigid-plastic finite element method. In :Transactions of ASME, Journal of Engineering Materials and Technology , vol 106,1984, p. 132-138
[7] Joshi, V.S.,Dixit,P.M.,Jain, V.K. Viscoplastic analysis of metal cutting by finite method .In : International Journal of Machine Tools and Manufacture, vol 34, 1994, p. 553-571.
[8] Kim, K.W.,Sin, H.C. Development of a thermo-viscoplastic cutting model using finite element method. In : International Journal of Machine Tools and Manufacture, vol 36, 1996, p. 379-397.
[9] Strenkowski, J.S.,Carrol, J.T. A finite element model of orthogonal metal cutting. In :Transactions of ASME, Journal of Engineering for Industry, vol 107,1985, p. 349-354
[10] Tugrul, O.,Altan, T. Process simulation using finite element method-prediction of cutting forces, tool stresses and temperatures in highspeed flat and milling. In : International Journal of Machine Tools and Manufacture, vol 40,2000,p.713-738.
[11] *** DEFORM 2DV 9.01.
[12] *** Manual 2D Machining Lab V90.
[13] *** SECO Tools Catalogue

MODELUL MECANIC AL PROCESULUI DE AŞCHIERE LA STRUNJIREA OŢELURILOR

Rezumat: In vederea imbunatatirii proceselor de aschiere a materialelor metalice este necesara aplicarea modelarii numerice si simularii acestora.O cerinta necesara este de a modela numeric interactiunea dintre interfata scula-aschie pentru a prezice performanta procesului de aschiere.Fortele de aschiere apar ca rezultat al deformarii elastice si plastice a aschiei si a suprafetei prelucrate , pentru ruperea , detasarea , deformarea suplimentara (incovoierea si spiralarea) a aschiei , precum si invingerea fortelor de frecare dintre aschie si fata de degajare si dintre fata de degajare si suprafata prelucrata.

Sorin ACHIMAŞ, PhD Student, Eng., Technical University of Cluj-Napoca, Department of Manufacturing Engineering, Muncii Bvd. 400641 Cluj-Napoca,E-mail: sorin_achimas@yahoo.com, Phone: 0040 264 426606.

Marian BORZAN, Univ. Prof. Dr. Eng., Technical University of Cluj-Napoca, Department of Manufacturing Engineering, Muncii Bvd. 400641 Cluj-Napoca, E-mail: Marian.Borzan@tcm.utcluj.ro, Phone: 0040 264 401647

Dorina (căs. BĂRĂIAN) PINTEA, PhD Student, Eng., Technical University of Cluj-Napoca, Department of Manufacturing Engineering, Muncii Bvd. 400641 Cluj-Napoca, Phone: 0040 264 401731.

Florin MOCEAN, PhD Student, Eng., Technical University of Cluj-Napoca, Department of Manufacturing Engineering, Muncii Bvd. 400641 Cluj-Napoca, Phone: 0040 264 401731.

Adrian TRIF, Lecturer.Dr. Eng., Technical University of Cluj-Napoca, Department of Manufacturing Engineering, Muncii Bvd. 400641 Cluj-Napoca, E-mail: adriantrif@tcm.utcluj.ro, Phone: 0040 264 401647